

Broad resistivity transitions in *c*-axis-in-plane-aligned *a*-axis-oriented $\text{YBa}_2\text{Cu}_3\text{O}_x$ thin films

Masashi Mukaida

Nippon Telegraph and Telephone LSI Laboratories, 3-1, Morinosato Wakamiya, Atsugi-shi, Kanagawa 243-01, Japan

(Received 8 April 1994)

The broadening of resistivity curves is measured for a *c*-axis-in-plane-aligned *a*-axis-oriented $\text{YBa}_2\text{Cu}_3\text{O}_x$ epitaxial thin film in the vicinity of the superconducting transition in magnetic fields up to 12 T with various current and magnetic-direction configurations. The direction of the magnetic field with respect to the crystallographic axis is the most important factor governing the broadening of the resistive transition. The direction of the current with respect to the crystallographic axis and to the magnetic-field direction is of less importance. Based on the results, flux-flow resistivity is extracted for the film in the 12-T magnetic field running parallel to the *c*-axis direction.

I. INTRODUCTION

One of the most significant features of high-critical-temperature (T_c) superconductors is the broadening of the resistivity transition in magnetic fields¹ over a wide temperature region below T_c . This broadening phenomenon was explained by the energy dissipation related to thermally activated flux creep and flux flow.²⁻⁶ Controversial results were reported by Kitazawa *et al.*⁷ using single-crystalline $(\text{La}_{1-x}\text{Sr}_x)_2\text{CuO}_4$, indicating that the broadening depends not on the magnetic-field direction with respect to the current direction but on the magnetic-field direction with respect to the crystallographic axis. This indicated that the broadening was due to non-flux-flow-type mechanisms. This finding was also followed in $\text{YBa}_2\text{Cu}_3\text{O}_x$ single crystals.^{8,9} However, the sample length along the *c* axis in $\text{YBa}_2\text{Cu}_3\text{O}_x$ single crystals is usually shorter by a few orders of magnitude than that along the *a* or *b* axes. Consequently, there remained some ambiguities in the transport properties with a current direction along the *c* axis.

On the other hand, the resistivity transition in the presence of a magnetic field showed a parallel shift in *c*-axis-oriented $\text{YBa}_2\text{Cu}_3\text{O}_x$ epitaxial thin films^{10,11} rather than the broadening observed in $\text{YBa}_2\text{Cu}_3\text{O}_x$ single crystals. This parallel shift was well explained in terms of a thermally activated flux-flow model by introducing the temperature-dependent pinning potential for the depinning of vortices. Here, the resistivity curves along the current direction of only the *ab* plane were observed. There were no resistivity curve measurements along the *c*-axis current direction.

Therefore, it is important to clarify the broad resistivity transitions along the *c* and *b* axes in the presence of a magnetic field in order to confirm the broadening mechanism of $\text{YBa}_2\text{Cu}_3\text{O}_x$. This paper reports on the broadening of resistivity curves by using *c*-axis-in-plane-aligned *a*-axis-oriented $\text{YBa}_2\text{Cu}_3\text{O}_x$ epitaxial thin films.¹² This is being observed for the first time in magnetic fields up to 12 T with various current and magnetic direction configurations.

II. EXPERIMENT

Thin films of $\text{YBa}_2\text{Cu}_3\text{O}_x$ were deposited on single-crystalline SrLaGaO_4 (100) substrates by a pulsed laser deposition method described earlier.¹² The films with a thickness of about 2700 Å, as measured using a mechanical stylus, were grown by a self-template technique.¹³ The axis of the films normal to the substrate surface were characterized by estimating lattice constants of the films, which were determined by x-ray diffraction (XRD) with $\text{Cu-K}\alpha$ radiation. In-plane alignment was confirmed by ϕ -scan (in-plane rotation) x-ray diffraction, reflection high-energy electron diffraction (RHEED), and planar, as well as cross-sectional-view transmission electron microscopy (TEM). The film was patterned into two 500- μm -long and 140- μm -wide rectangular lines along the *b* axis and along the *c* axis with four electrodes for the four-probe method. The current density to measure the resistivity was 26.5 A/cm² and 132.3 A/cm² for the current direction along the *c* axis and along the *b* axis, respectively. The magnetic field was applied with a superconducting solenoid using a rotating sample holder. The temperature was determined with a carbon glass thermometer with detailed correction for the magnetoresistance.¹⁴

III. RESULTS AND DISCUSSIONS

A. Crystal structures

Samples used in this experiment were $\text{YBa}_2\text{Cu}_3\text{O}_x$ thin films on SrLaGaO_4 (100) substrates. Since the electrical properties strongly depend on the quality of the sample, the crystalline structure of the film was estimated in detail. A typical x-ray-diffraction pattern of as-grown $\text{YBa}_2\text{Cu}_3\text{O}_x$ thin films is shown in Fig. 1. Peaks are observed at around 23° and around 47.6°. The lattice spacing of these peaks was 3.82(0) Å, which is considered to be the same as that for (*h*00) peaks of the $\text{YBa}_2\text{Cu}_3\text{O}_x$. Then the $\text{YBa}_2\text{Cu}_3\text{O}_x$ thin films were determined to be *a*-axis oriented.

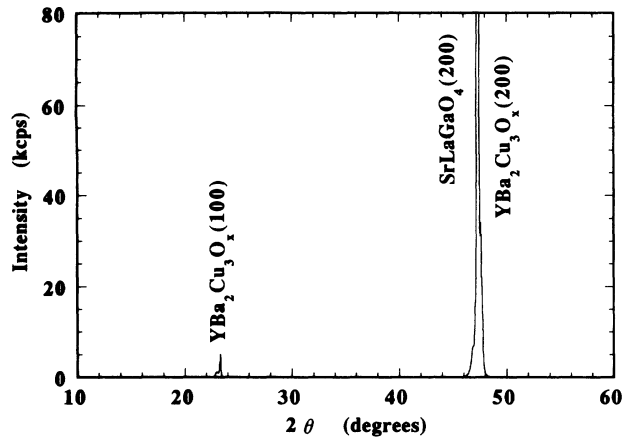


FIG. 1. A typical x-ray-diffraction pattern of $\text{YBa}_2\text{Cu}_3\text{O}_x$ thin films on SrLaGaO_4 (100) substrates. The films were determined to be *a*-axis oriented.

Figure 2 shows RHEED patterns for $\text{YBa}_2\text{Cu}_3\text{O}_x$ thin films aligned to the $\langle 010 \rangle$ [Fig. 2(a)] and $\langle 001 \rangle$ [Fig. 2(b)] azimuths of the substrate. A RHEED pattern corresponding to the characteristic trilayer structure of $\text{YBa}_2\text{Cu}_3\text{O}_x$ is clearly observed in the direction of the $\langle 010 \rangle$ azimuth for the substrate [Fig. 2(a)], while no such pattern is observed along that direction for the $\langle 001 \rangle$ azimuth [Fig. 2(b)]. These results suggest that the *c* axis for the grown *a*-axis-oriented thin film is aligned in-plane to the $\langle 001 \rangle$ azimuth for the (100) SrLaGaO_4 substrate. The same result was obtained by ϕ -scan measurements.¹²

Actually, planar view TEM images of the *a*-axis oriented $\text{YBa}_2\text{Cu}_3\text{O}_x$ thin films revealed that the *c* axis of the film was aligned one direction as shown in Fig. 3. Therefore, the films were confirmed to be *c*-axis-in-plane-aligned *a*-axis-oriented $\text{YBa}_2\text{Cu}_3\text{O}_x$ thin films.

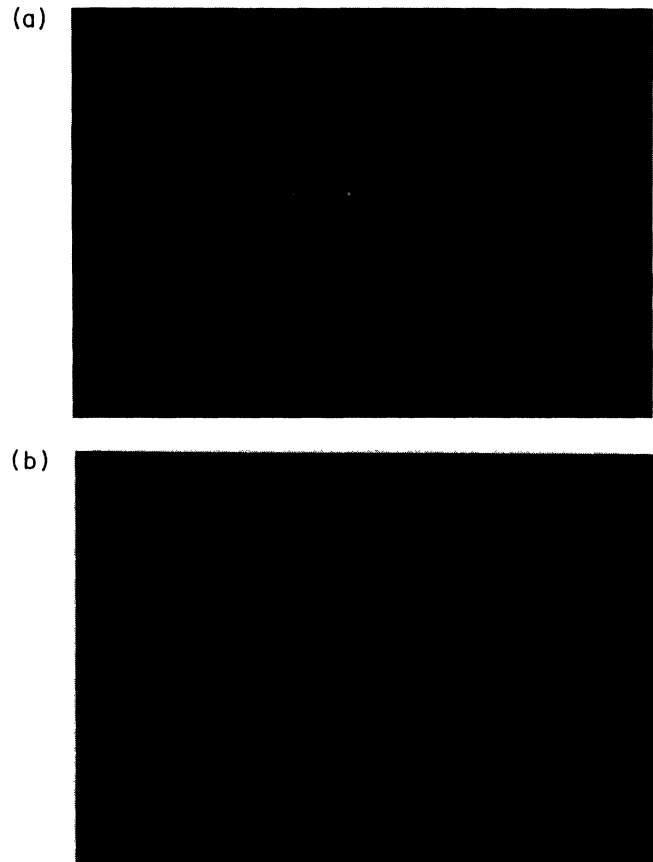


FIG. 2. RHEED pattern of the $\text{YBa}_2\text{Cu}_3\text{O}_x$ films on SrLaGaO_4 (100) substrates with (a) $\langle 010 \rangle$ SrLaGaO_4 incident beam azimuth and (b) $\langle 001 \rangle$ SrLaGaO_4 incident beam azimuth. RHEED patterns associated with a trilayer structure were observed only in the $\langle 010 \rangle$ SrLaGaO_4 incident beam azimuth.

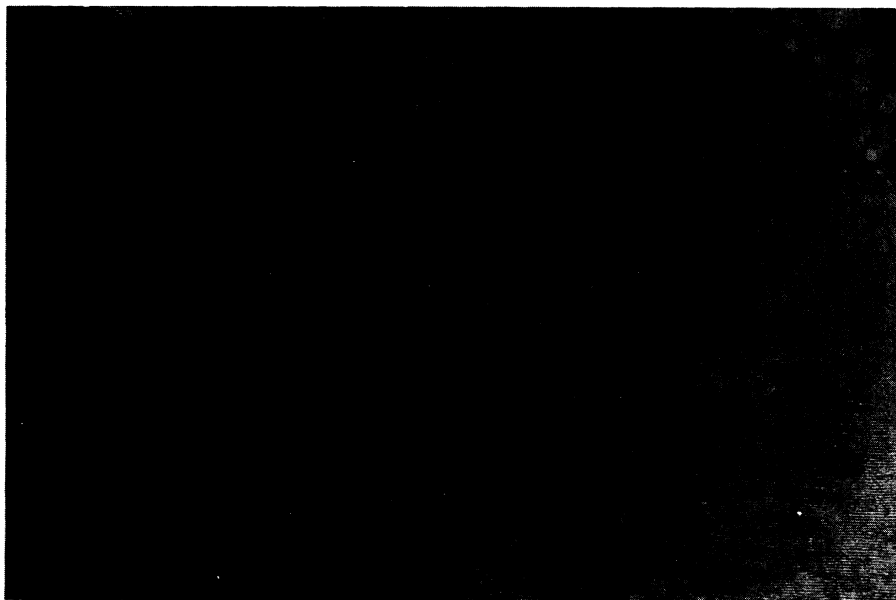


FIG. 3. A planar-view transmission electron microscopy image. The Cu-oxygen planes are clearly observed that they are aligned in one direction, which is the $\langle 010 \rangle$ substrate azimuth.

500Å

B. Electrical properties

The zero-magnetic-field resistivity curves over the whole temperature range below 300 K are shown in Fig. 4 for both current directions along the c axis (a) and along the b axis (b). The temperature dependence of the normal-state resistivity is different between the two crystallographic orientations. The temperature dependence of the resistivity with the current along the b axis is more metallic than that along the c axis, resulting in a large resistivity difference. The resistivity in the c -axis direction is 24 times larger than that in the b -axis direction (anisotropy: $\gamma^2=24$) at a point just above the transition temperature (95 K).

The resistivity curves in magnetic fields along the a axis are shown in Fig. 5 with the current direction along the c axis (a) and along the b axis (b). The resistivity curves in magnetic fields along the c axis are shown in Fig. 6 with the current direction along the c axis (a) and along the b axis (b). The resistivity broadening in (a) and (b) in the figures corresponds to the current direction running parallel to the c axis and to the b axis, respectively. The resistivity broadening in Fig. 5, where the magnetic field runs parallel to the a axis, is much smaller than that in Fig. 6, where the field runs parallel to the c axis. Notice that a high degree of broadening was observed when the magnetic field direction was along the c axis, independent of the current directions. From this, it was concluded that the direction of the magnetic field with respect to the crystallographic axis was the most important factor governing the broadening of the resistivity transition. These results were similar to those of $(\text{La}_{1-x}\text{Sr}_x)_2\text{CuO}_4$ single crystals⁷ and $\text{YBa}_2\text{Cu}_3\text{O}_x$ single crystals.⁸ The direction of the current with respect to the crystallographic axis and with respect to the magnetic-field direction is of less importance. The experimental data are difficult to understand within a standard flux-flow model.

There were some reports explaining this broadening by intrinsic Josephson coupling between two-dimensional strong superconducting planes.^{15,16} In these explana-

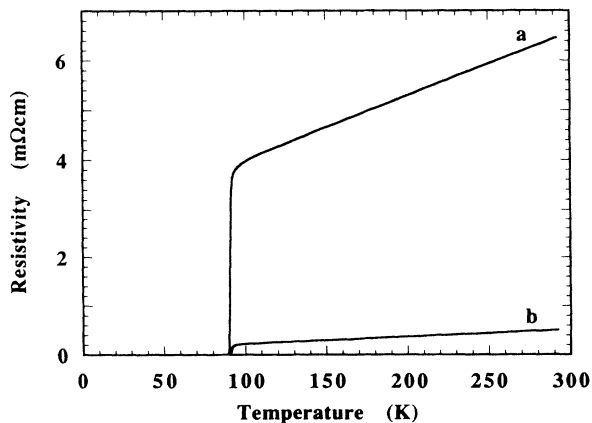


FIG. 4. Zero-magnetic-field resistivity curves of c -axis-in-plane-aligned a -axis-oriented $\text{YBa}_2\text{Cu}_3\text{O}_x$ epitaxial thin film (a) along the c axis and (b) along the b axis. These samples were prepared from the same film.

tions, the CuO_2 plane is assumed to be a strong superconductor and the CuO chain is assumed to be a weak superconductor in $\text{YBa}_2\text{Cu}_3\text{O}_x$. As a result of proximity effects from the adjacent strong superconductor, the resistivity transition broadening in the perpendicular configuration of $I \perp B$ [Fig. 5(a)], where Josephson vortices are driven along the b axis in the weak superconductor by the Lorentz force, should have been a broad transition. However, it is not broad but instead is almost the same as that in Fig. 5(b), where vortices are driven along the c axis, against the strong superconductor of the CuO_2 planes by the Lorentz force. This makes it difficult to explain the broadening by citing intrinsic Josephson coupling and/or the anisotropy of the superconductors.

This phenomenon has been explained qualitatively by vortex lattice melting in the CuO_2 planes. When vortex lattice melting occurs in the $\text{YBa}_2\text{Cu}_3\text{O}_x$ films, a large flux-flow resistivity should have appeared. Figure 7

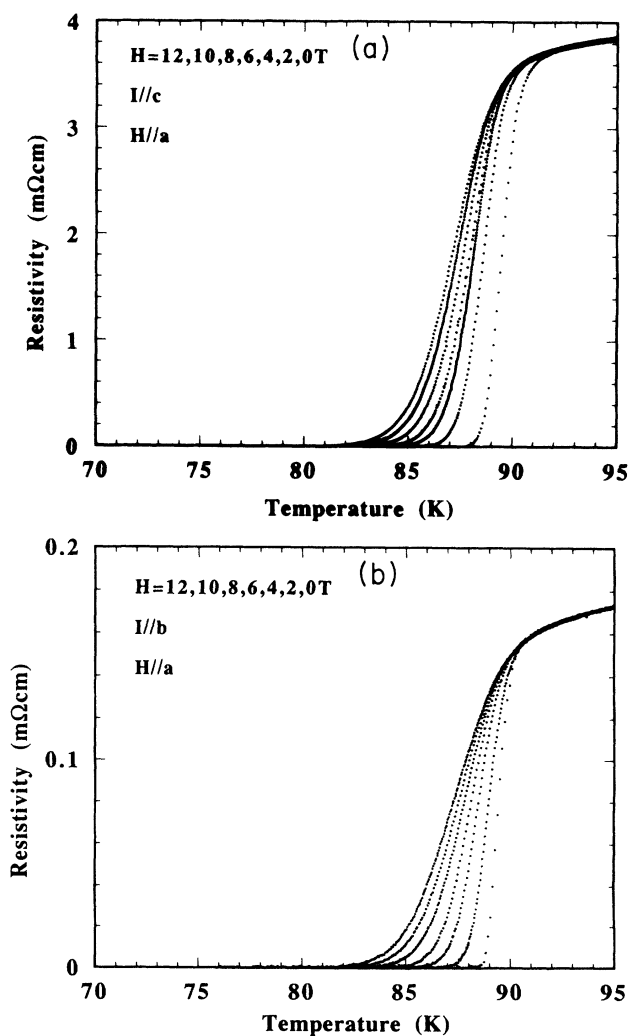


FIG. 5. The resistivity curves of c -axis-in-plane-aligned a -axis-oriented $\text{YBa}_2\text{Cu}_3\text{O}_x$ epitaxial thin film in the vicinity of the superconducting transition for different values of the magnetic field parallel to the a axis with various magnetic-field current configurations; from right to left 0, 2, 4, 6, 8, 10, and 12 T; (a) $I \parallel c$ axis, $B \parallel a$ axis, and $I \perp B$; (b) $I \parallel b$ axis, $B \parallel a$ axis, and $I \perp B$.

shows the normalized resistivity curves (ρ) in a 12 T magnetic field running parallel to the *c* axis for different current directions at 90 K. The precise comparison between the two curves reveals a small Lorentz-force-induced flux-flow resistivity shoulder with a perpendicular configuration of $\mathbf{I} \perp \mathbf{B}$. The difference between two curves was thought to be flux-flow resistivity. The flux-flow resistivity ($\rho_b - \rho_c$) could be extracted from the curves as shown in Fig. 7, where ρ_b and ρ_c correspond to the normalized resistivity with the current direction running parallel to the *b* axis and to the *c* axis, respectively. It was found that the flux-flow resistivity had a peak at around 79 K and was induced from 73 K by Lorentz force in this sample. The shoulders can also be seen in Fig. 6(b) with a magnetic field. These shoulders are very small compared to those observed in $\text{YBa}_2\text{Cu}_3\text{O}_x$ single crystals, indicating a strong pinning force in the $\text{YBa}_2\text{Cu}_3\text{O}_x$ films.

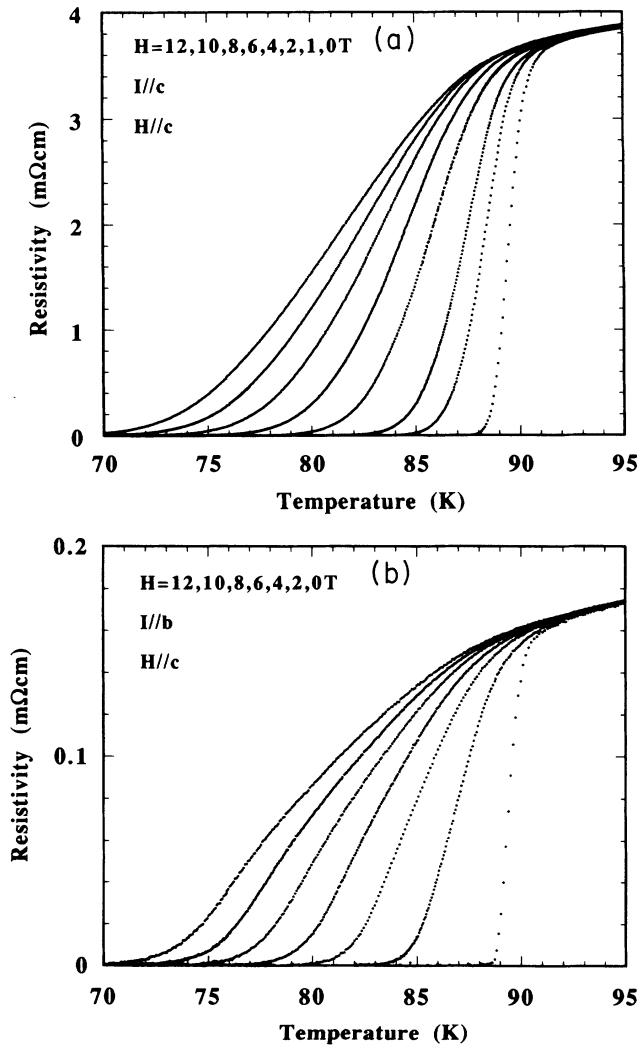


FIG. 6. The resistivity curves of *c*-axis-in-plane-aligned *a*-axis-oriented $\text{YBa}_2\text{Cu}_3\text{O}_x$ epitaxial thin film in the vicinity of the superconducting transition for different values of the magnetic field parallel to the *c* axis with various magnetic-field current configurations; from right to left 0, 1, 2, 4, 6, 8, 10, and 12 T; (a) $\mathbf{I} \parallel \mathbf{c}$ axis, $\mathbf{B} \parallel \mathbf{c}$ axis, and $\mathbf{I} \parallel \mathbf{B}$; (b) $\mathbf{I} \parallel \mathbf{b}$ axis, $\mathbf{B} \parallel \mathbf{c}$ axis, and $\mathbf{I} \perp \mathbf{B}$.

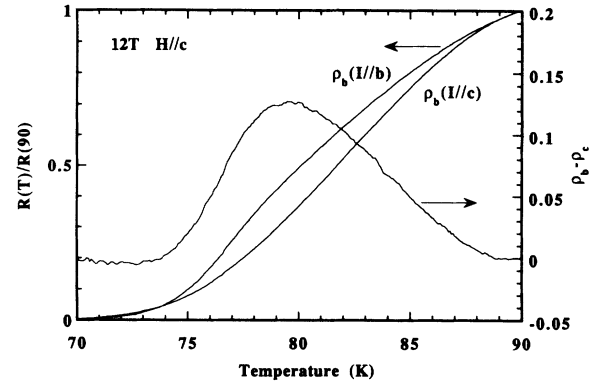


FIG. 7. The normalized resistivity curves in the vicinity of the superconducting transition for different current directions (ρ_b , *b* axis; ρ_c , *c* axis) in a 12-T magnetic field parallel to the *c* axis. Besides the flux-flow resistivity, broadening is almost the same in both the ρ_b and ρ_c . Flux-flow resistivity was calculated as $\rho_b - \rho_c$.

Therefore, it is also difficult to explain the broadening by citing vortex lattice melting in $\text{YBa}_2\text{Cu}_3\text{O}_x$ films with a strong pinning force.

Besides this small shoulder, the resistivity curves are almost the same. This result is thought to imply that the broadening mechanism is clearly related to the direct contribution of the magnetic field to the quasi-two-dimensional Fermi surface of $\text{YBa}_2\text{Cu}_3\text{O}_x$.

IV. CONCLUSIONS

The resistivity curves for four different configurations between the current and the magnetic-field directions with respect to the crystallographic axes were measured in the vicinity of the superconducting transition in magnetic fields up to 12 T using *c*-axis-in-plane-aligned *a*-axis-oriented $\text{YBa}_2\text{Cu}_3\text{O}_x$ epitaxial films. The direction of the magnetic field with respect to the crystallographic axis was determined to be the most important factor that governs the broadening of the resistive transition. The less important current direction with respect to the magnetic field direction clearly indicated that the less important flux-flow effect induced by a Lorentz force than the intrinsic magnetic field effect on the quasi-two-dimensional Fermi surface of the oxide high- T_c cuprate superconductors. Flux-flow resistivity was extracted by comparing the normalized resistivity with the perpendicular configuration of $\mathbf{I} \perp \mathbf{B}$ to that of the parallel configuration of $\mathbf{I} \parallel \mathbf{B}$.

ACKNOWLEDGMENTS

The author would like to acknowledge Dr. Shintaro Miyazawa of NTT LSI Laboratories, Dr. Minoru Suzuki of NTT Interdisciplinary Laboratories, and Dr. Susumu Kurihara, Dr. Kouichi Semba, and Dr. Masao Naito of NTT Basic Research Laboratories for their valuable comments and for discussions, and Dr. Kazuo Kadowaki of National Research Institute for Metals for valuable discussions.

- ¹ Y. Iye, T. Tamegai, H. Takeya, and H. Takei, *Jpn. J. Appl. Phys.* **26**, L1057 (1987).
- ² Y. Yeshurun and A. P. Malozemoff, *Phys. Rev. Lett.* **60**, 2022 (1988).
- ³ M. Tinkham, *Phys. Rev. Lett.* **61**, 1658 (1988).
- ⁴ T. T. M. Palstra, B. Batlogg, L. F. Schneemeyer, and J. V. Waszczak, *Phys. Rev. Lett.* **61**, 1662 (1988).
- ⁵ T. T. M. Palstra, B. Batlogg, R. B. van Dover, L. F. Schneemeyer, and J. V. Waszczak, *Appl. Phys. Lett.* **54**, 763 (1989).
- ⁶ W. K. Kwok, U. Welp, G. W. Crabtree, K. G. Vandervoort, R. Hulscher, and J. Z. Liu, *Phys. Rev. Lett.* **64**, 966 (1989).
- ⁷ K. Kitazawa, S. Kambe, M. Naito, I. Tanaka, and H. Kojima, *Jpn. J. Appl. Phys.* **28**, L555 (1989).
- ⁸ J. N. Li, K. Kadowaki, M. J. V. Menken, A. A. Menovsky, and J. J. M. Franse, *Physica C* **161**, 313 (1989).
- ⁹ K. Kadowaki, J. N. Li, and J. J. M. Franse, *Physica C* **170**, 298 (1990).
- ¹⁰ C. T. Rogers, S. Gregory, T. Venkatesan, B. Wilkens, X. D. Wu, A. Inam, B. Dutta, and M. S. Hegde, *Appl. Phys. Lett.* **54**, 2038 (1989).
- ¹¹ M. Suzuki, H. Asano, and S. Kubo, *Jpn. J. Appl. Phys.* **32**, L723 (1993).
- ¹² M. Mukaida and S. Miyazawa, *Appl. Phys. Lett.* **63**, 999 (1993).
- ¹³ O. Nakamura, J. Guimple, F. Sharifi, R. C. Dynes, and I. K. Schuller, *Appl. Phys. Lett.* **61**, 2598 (1992).
- ¹⁴ H. H. Sample, *Rev. Sci. Instrum.* **58**, 1129 (1982).
- ¹⁵ W. Lawrence and S. Doniach, *Proceedings of the 12th International Conference on Low Temperature Physics, Kyoto, 1970*, edited by E. Kanda (Academic Press of Japan, Kyoto, 1971), p. 361.
- ¹⁶ G. Oya, N. Aoyama, A. Irie, S. Kishida, and H. Tokutaka, *Jpn. J. Appl. Phys.* **31**, L829 (1992); K. Kadowaki (private communication).

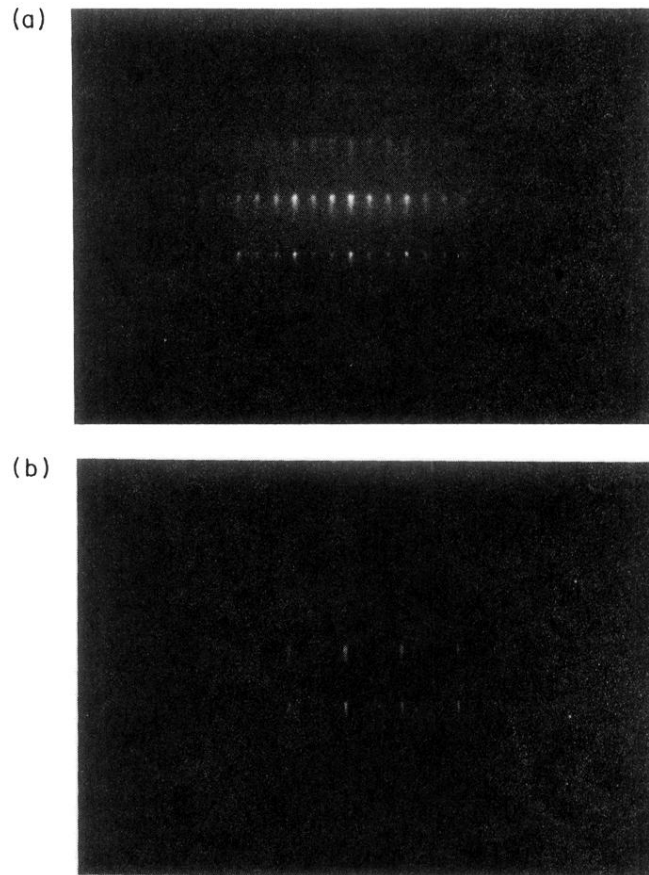


FIG. 2. RHEED pattern of the $\text{YBa}_2\text{Cu}_3\text{O}_x$ films on SrLaGaO_4 (100) substrates with (a) $\langle 010 \rangle$ SrLaGaO_4 incident beam azimuth and (b) $\langle 001 \rangle$ SrLaGaO_4 incident beam azimuth. RHEED patterns associated with a trilayer structure were observed only in the $\langle 010 \rangle$ SrLaGaO_4 incident beam azimuth.

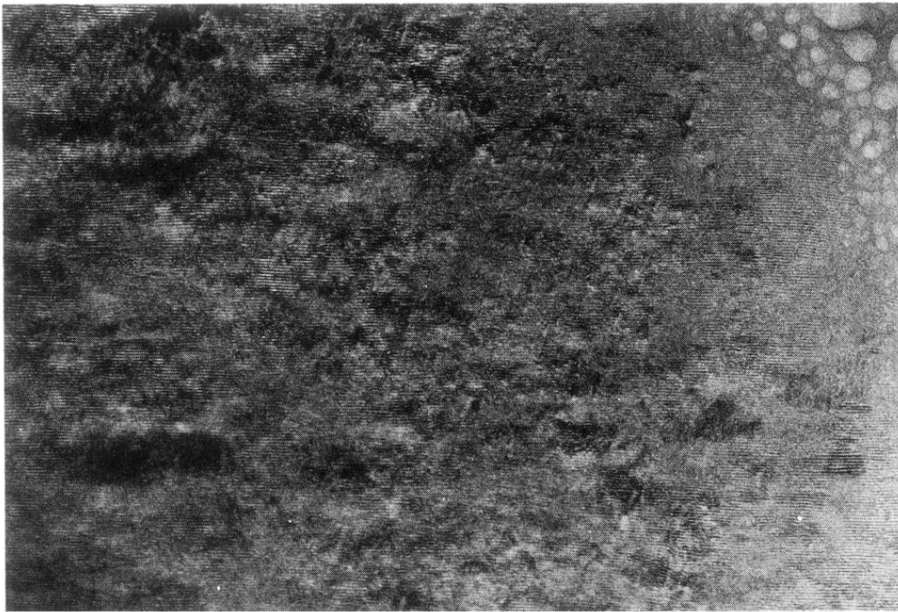


FIG. 3. A planar-view transmission electron microscopy image. The Cu-oxygen planes are clearly observed that they are aligned in one direction, which is the $\langle 010 \rangle$ substrate azimuth.

↔
500Å